

表① これまで行われてきた主な Cell based gene therapy

報告者	Cell	Gene	対象	導入部位	目的
1 Plautz, G. et al <sup>9)</sup>	SMCs (smooth muscle cell)	$\beta$ -galactosidase	動脈壁	腸骨動脈	組み換え遺伝子による血管病変の治療
2 Forough, R. et al <sup>10)</sup>	SMCs (smooth muscle cell)	TIMP-1	障害血管	内頸動脈	内皮細胞の過形成を防ぐ
3 Chen, L. et al <sup>11)</sup>	SMCs (smooth muscle cell)	ecNOS	障害血管	内頸動脈	内皮の変性を抑える, 血管内腔の拡張の制御
4 Osborne, W.R.A. et al <sup>12)</sup>	SMCs (smooth muscle cell)	Epo	内頸動脈	内頸動脈	赤血球の増加
5 Nabel, E. et al <sup>13)</sup>	Endothelial cell	recombinan DNA	障害血管	腸骨動脈	血栓溶解, 血管新生, 成長因子の発現
6 Messina, L. et al <sup>14)</sup>	Endothelial cell	lac Z	虚血四肢	大腿動脈	骨格筋への内皮細胞の導入
7 Willson, J. et al <sup>15)</sup>	Endothelial cell	lac Z	動脈硬化症	グラフト	動脈硬化症の治療
8 Dichek, D.A. et al <sup>16)</sup>	Endothelial cell	TPA, a-UPA	人工血管グラフト	大腿動脈, 内シヤント	抗血栓効果
9 Flugelman, M.Y. et al <sup>17)</sup>	Endothelial cell	t-PA	ステント	ステント	血栓溶解
10 Koh, G.Y. et al <sup>18)</sup>	skeletal myoblast	TGF- $\beta$	心筋	心筋	局所での組み換え分子の長期発現
11 Barr, E. et al <sup>19)</sup>	myoblast	human growth hormone	正常下肢	下肢筋肉	循環中への安定したタンパク導入
12 Lee, R.J. et al <sup>20)</sup>	myoblast	VEGF	正常心筋	左室壁	血管新生に調節された血管新生因子の発現が必要
13 Yau, T.M. et al <sup>21)</sup>	myocardial cell	VEGF	虚血心筋	心筋虚血部	血管新生
14 Suzuki, K. et al <sup>22)</sup>	skeletal myoblast	VEGF	虚血心筋	心筋虚血部	血管新生, 血管拡張
15 Lu, Y. et al <sup>23)</sup>	bioartificial muscle	VEGF	虚血四肢	虚血四肢	血管新生・タンパク運搬
16 Campbell, A.I.M. et al <sup>24)</sup>	SMCs (smooth muscle cell)	VEGF	肺高血圧症	内頸静脈	肺高血圧症の進展を防ぐ・右室リモデリングの改善
17 Iwaguro, H. et al <sup>25)</sup>	EPCs	VEGF	虚血四肢	尾静脈	血管新生・血流改善

よりよい血管新生療法には有用な血管新生因子が必要であり, 導入する血管新生因子としてこれまでに FGF (fibroblast growth factor), VEGF (vascular endothelial growth factor)<sup>[用語解説2]</sup>, HGF (hepatocyte growth factor), EGF (epidermal growth factor), PDGF (platelet-derived growth factor) などが報告されている<sup>3) 4)</sup>.

1992年, Baffourら<sup>5)</sup>により家兎の下肢虚血モデルに対しFGF-2を導入することではじめて血管新生因子を用いた血管新生療法が報告された。その後もVEGFを用いた血管新生療法の有効性が報告されたが, これらは遺伝子導入ではなく直接タンパクを導入するものであった。ヒトへの臨床応用を考えると大量のタンパク質の精製に莫大なコストがかかる。そのため血管新生因子のプラスミドを血管内あるいは虚血部に投与する遺伝子治療が考えられた。

これら血管新生因子は血管内皮細胞増殖作用だけでなく様々な生物活性作用も有する。しかしながらこれらの血管新生因子が実際の生体における血管新生時にどのように関与しているかわかっていない。

最近の研究では血管新生因子の発現による血管新生<sup>[用語解説3]</sup>の過程が明らかになりつつあり, VEGFの過剰発現により腫瘍形成や血管透過性の

高い新生血管の発育などが報告されている。正常な血管新生と成熟した血管の発育には細胞の型と分子のバランスが必要であるという Well-tempered vessel の概念<sup>6)</sup> が提唱されており, そのためには相互に調節しあった血管新生因子, 細胞や遺伝子を組み合わせたハイブリッド治療<sup>7)</sup>が必要となってくると考えられる。生分解性ゼラチンを用いた遺伝子導入療法は, *in vitro*での細胞内への遺伝子導入を非ウイルスベクターで高効率に行うことができ, 両親媒性ベクターとして血管内投与の可能な非侵襲性治療が期待できる優れた方法であり, さらに治療効果に関連する機能を有する複数の因子を導入することで細胞の作用と遺伝子の作用の相乗効果のみならず, それぞれの補完性も合わせ持った治療が可能となるであろう。

## II. Cell-based gene therapy<sup>8) - 24)</sup>

Cell-basedの遺伝子導入療法は, 遺伝子の発現期間の延長を通じて well-tempered vessel の形成に役立つ可能性がある<sup>8)</sup>。1991年にPlautzら<sup>9)</sup>によりはじめてCell-basedの遺伝子導入が行われ, それ以降平滑筋や内皮細胞を用いた遺伝子導入が報告されてきた。その目的は遺伝子単独導入療法に比べて, より安定した, また長期の遺伝子発現

である。その目的のために種々の細胞を遺伝子発現の基地 (base) として用いる。細胞内ではDNA分解酵素による遺伝子の分解は極めて限られており、一方、遺伝子の転写からタンパクの発現にいたる全ての機構が整えられている。これらの理由から *ex vivo* で細胞内に遺伝子を導入し、この細胞を生体内に投与するという cell-based gene therapy<sup>9)-25)</sup> が行われるようになった。

表①に示すようにbaseとして用いられる細胞としては内皮細胞<sup>13)-17)</sup>、骨格筋細胞<sup>19)-23)</sup>、平滑筋細胞<sup>9)-12)</sup><sup>24)</sup>などが報告されている。遺伝子治療の標的器官は心臓、肺、下肢などである。導入される遺伝子はVEGFなどの血管新生因子<sup>20)-25)</sup>、GFPなどのマーカー遺伝子<sup>9)</sup>、その他の遺伝子(TIMP-1<sup>10)</sup>、t-PA<sup>9)</sup>、ecNOS<sup>11)</sup>)などが報告されている。

Cell-basedの遺伝子導入の利点は、

- (1)障害血管へ選択的な遺伝子導入を行うために、人工血管やステントのコーティングとして細胞を用いる。全身投与の手段としても用いられる可能性を有する。
- (2)遺伝学的に細胞を比較的均一な集団として発育させることができる。
- (3)遺伝子の導入、発現が確実に行われる。
- (4)ベクターに対する免疫、炎症反応が少ない、などである。

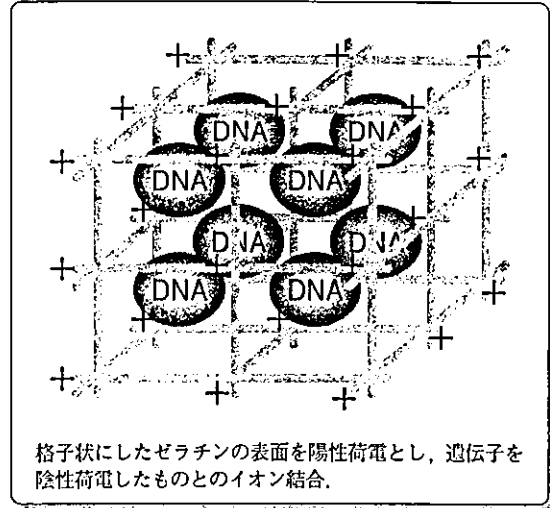
逆に、

- (1)発現に遅れが伴う。
- (2)採取、植え込みに別の過程が必要である。
- (3)同系の細胞が必要である。
- (4)培養中に細胞の表現型の変化が起こる、などの欠点もある。

遺伝子導入の標的細胞として当初血管系、平滑筋細胞と内皮細胞を使って行われた。血管内皮細胞は局所での血管の状態を調節し全身への遺伝子投与という可能性を持っている。

Plautz<sup>9)</sup>らによる平滑筋細胞にβ-galactosidaseを遺伝子導入した研究を皮切りに、いくつかの研

図① 生分解性ゼラチンの格子構造—遺伝子結合



究が行われた。Forough<sup>10)</sup>らはTIMP-1を導入し内膜の過形成を減少させ、Chen<sup>11)</sup>らはeNOSを導入することにより血管のリモデリング、血管径の拡張を起こさせた。さらにはエリスロポイエチンの導入による赤血球の増加、血管新生などへの可能性に研究も行われた。

内皮細胞は微小血管のネットワークに接着するので、骨格筋の血管床なども遺伝子投与のレシピエントとなる利点を持っている。

内皮細胞への遺伝子導入<sup>13)-15)</sup>は、全身への遺伝子投与の手段として始められ、グラフト<sup>16)</sup>や、t-PAを導入したステントへの細胞-遺伝子導入<sup>17)</sup>なども行われた。

しかし、ほとんどのCell-based gene therapyの場合、細胞の役割は、基地・baseとしての機能であり細胞自体による治療効果は一部を除いて考慮されていなかった。また大部分の遺伝子を導入した細胞は血管内投与で用いることはできなかった。細胞塊が血管を閉塞する危険性があるためである。そのため胸、腹部の主要臓器への投与はかなりの侵襲を伴うこととなる。

### III. ゼラチンを用いた遺伝子細胞ハイブリッド治療

本治療法は以下のような特徴を有する。

- (1)cellがbaseとしてだけでなく治療要素としての働きを持つ

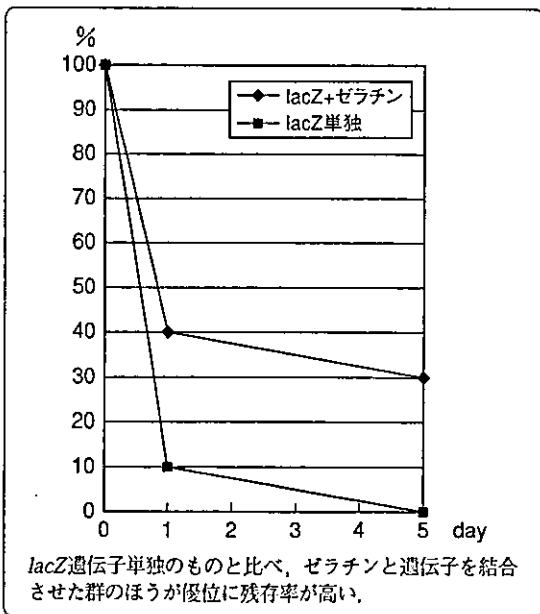
- (2)血管内投与が可能である  
 (3)ex vivoでの導入効果が高い  
 などの点で、従来のcell-based gene therapyよりも優れている。

このハイブリッド治療を実現するkeyとなる物質がゼラチンである(図①)。

ゼラチンの特徴として、

- (1)陽性に帯電しているのに陰性に帯電している種々の物質(核酸やタンパク質)をイオン結合することができる。
- (2)構造が三次元格子状なので結合物質をゲル内部に保護することにより分解酵素の影響を受けにくくする。
- (3)ゼラチンであるため生体内で徐々に分解を受けて、この分解に伴い結合物質を放出する。
- (4)その分解速度は架橋度を変えることにより自由に調節できる。
- (5)ゼラチン-遺伝子複合体は貪食細胞(血管内皮前駆細胞<sup>[用語解説4]</sup>、単球、マクロファージ)などに容易に貪食される。
- (6)貪食細胞内で高率に遺伝子を発現する。などが挙げられる。

図② 生体内におけるlacZ遺伝子残存率

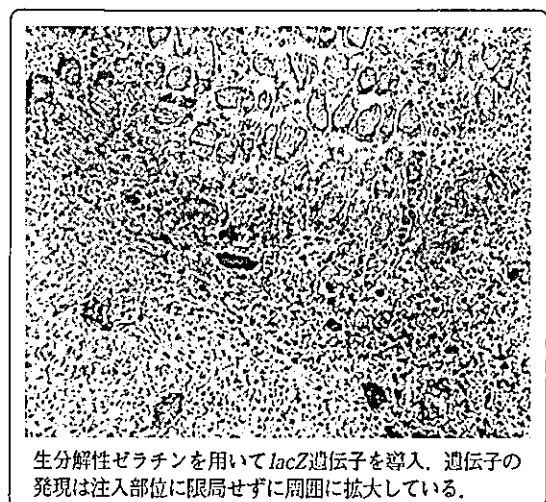


その構造や表面電荷を変えることが容易であることから<sup>26)</sup>、われわれはゼラチンを遺伝子の担体として利用することを着想した。そこでゼラチンの構造を格子状にしてその表面電荷を陽性とすることで陰性荷電した遺伝子とイオン結合させ、ゼラチン-遺伝子複合体を作成した。遺伝子をあらかじめゼラチンの格子構造内へ封入して生体内へ投与することで核酸分解酵素による遺伝子の代謝が緩徐となり、結果として安全かつ高効率に遺伝子を導入することができると考えられる。実際に遺伝子をゼラチンと結合させて投与したところ、生体内における遺伝子の残存期間を飛躍的に延長させることに成功し(図②)、遺伝子の発現率も従来の遺伝子の単独投与と比較して約10倍の増加が認められた(図③)<sup>27)</sup>。

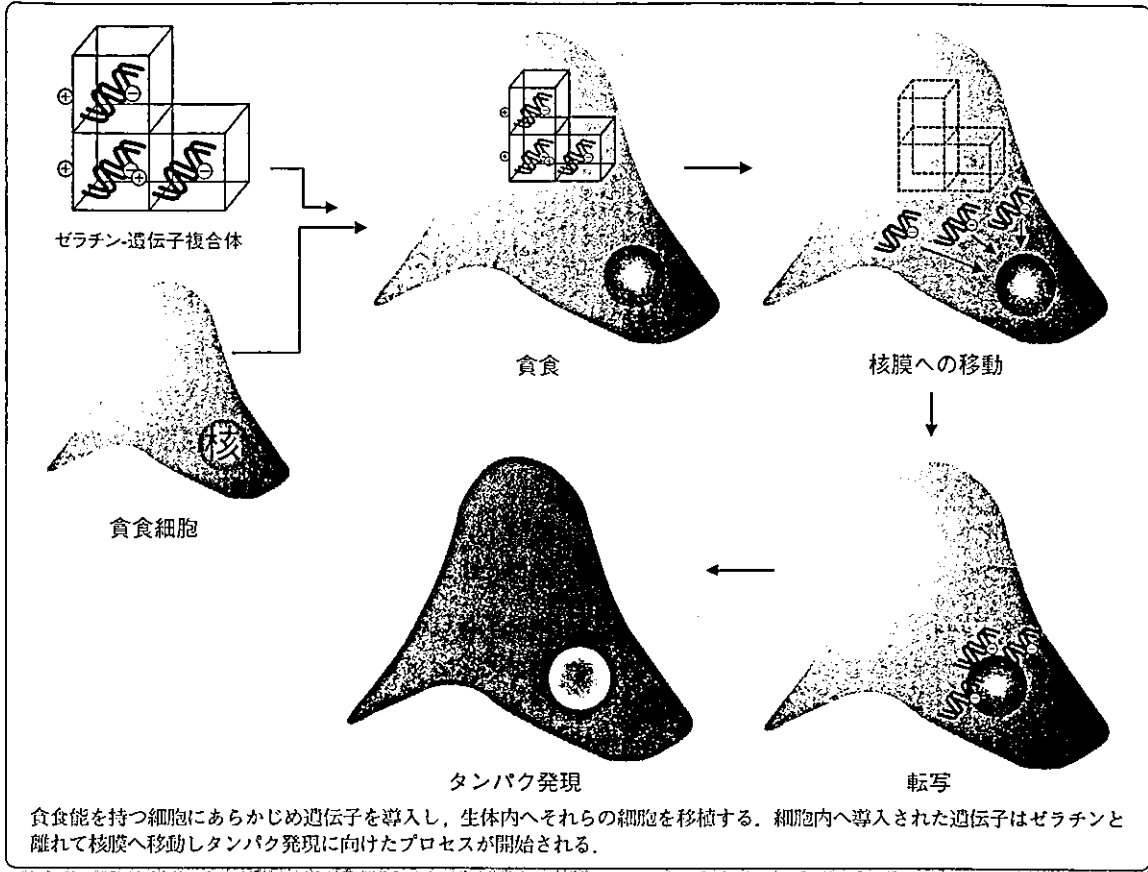
本法の優れた点は、ウイルスベクターを用いないため感染の危険性が少ないことに加えて、移植したマクロファージや単球が走化性によって障害部位に特異的に集まるため遺伝子の導入効率が高まること、また標的組織へ凝集したこれらの細胞が導入された遺伝子をもとにタンパク質を合成することである。

われわれが考案したゼラチンを用いた細胞内遺伝子導入法は、貪食能をもつ細胞であれば基本的

図③ 生分解性ゼラチン-lacZ



図④ 貪食細胞によるゼラチン-遺伝子複合体の取り込み



応用編

正章

再生医療とDDS

に適用可能であると考えられる。従って、貪食能を有する血管内皮細胞、マクロファージなどにあらかじめ遺伝子を導入して生体内へ細胞移植すれば、血管新生能力、標的細胞への遊走能に加えて導入した遺伝子による血管新生作用の相乗効果が期待される。下肢虚血モデルに対する治療法としては、機能強化の目的で血管内皮前駆細胞へ VEGF の遺伝子を導入して投与方法が報告され良好な成績が報告されている。(図④)

さらにわれわれは、血管内皮前駆細胞の有する血管新生作用と補完的な作用を有する遺伝子を導入することで、より成熟した血管床を再構築することをめざしており、難治性の循環障害である心筋梗塞、慢性閉塞性動脈硬化症、原発性肺高血圧症の治療に適用できないかと考えた。原発性肺高血圧症は何らかの原因により肺血管抵抗の上昇が起こり、その結果として右心不全が生じる病態であり、血管内皮細胞の機能不全が本病態の素因である可能性が指摘されており、現在の治療法とし

ては血管拡張物質である NO，プロスタサイクリン，アドレノメデュリンの治療効果が確認されている。

現在われわれはこれらの遺伝子を導入した血管内皮前駆細胞を用い、ラットの肺高血圧症モデルに対する細胞移植治療の効果を検討中であるが良好な成果を上げている<sup>28)</sup>。

## おわりに

以上よりゼラチンを用いた遺伝子導入による血管新生療法は、徐放化による持続発現のみならず、遺伝子・細胞それぞれの機能を生かした方法であるといえる。従来法に比べて、安全性、侵襲に関しても優れていると考えられるが、今後は遺伝子導入効率の改善はもとより、遺伝子の発現部位や発現時期を制御する技術も必要であろう。機能的により成熟した組織や器官の再生を可能とするには複数の細胞や遺伝子を組み合わせるハイブリッ

ド治療が必要であり、生分解性ゼラチンを用いた遺伝子導入法がヒトへの臨床応用へ向けてさらなる改善が必要となる。

●関連研究Web site

- www.ncvc.go.jp/  
国立循環器病センター
- http://www.nacos.com/jshc/  
日本組織細胞化学会
- http://new.nacos.com/jsch/  
日本細胞生物学会
- http://jtca.umin.jp/  
日本組織培養学会

用語解説

1. 血管形成 (vasculogenesis) 未分化な細胞(血管内皮前駆細胞)がin site(目的地)にて増殖、分化し血管を構成する過程。
2. VEGF (vascular endothelial growth factor: 血管内皮成長因子) 受容体が内皮細胞に発現するサイトカインで、血管周囲の細胞から産生・分泌される。血管内皮細胞を特異的に増殖させ、血管透過性を亢進させる活性をもつ。ヒト組織中に最も豊富にあるVEGF165はヘパリン結合性の分泌型糖タンパク質である。
3. 血管新生 (angiogenesis) 既存血管の血管内皮細胞が増殖および遊走して成立する成熟個体の血管形成。
4. 血管内皮前駆細胞 末梢血液中に存在する骨髓由来の細胞で、血管内皮細胞に分化可能な血液細胞として発見される。抗原性などから、胎児期に存在するangioblastに近い細胞と推察されている。生体の血管形成に血液中から患部に集積する。

▶▶参考文献

- 1) Isner JM, Pieczek A, et al: Lancet 348, 370-374, 1996.
- 2) Yang Y, Trinchieri G, et al: Nat Med 1, 890-893, 1995.
- 3) Gospodarowicz D, Brown KD, et al: J Cell Biol 77, 774-778, 1978.
- 4) Keck PJ, Hauser SD, et al: Science 246, 1309-1312, 1989.
- 5) Baffour R, Berman J, et al: J Vasc Surg 16, 181-191, 1992.
- 6) Blau HM, Banfi A, et al: Nat Med 7, 532-534, 2001.
- 7) 福山直人, 笠原啓史 他: 循環器科 51, 259-263, 2002.
- 8) Kullo JI, Simari DR, et al: Arterioscler Thromb Vasc Biol 19, 196-207, 1999.
- 9) Plautz G, Nabel EG, et al: Circulation 83, 578-583, 1991.

- 10) Forough R, Koyama N, et al: Circ Res 79, 812-820, 1996.
- 11) Chen L, Daum G, et al: Circ Res 82, 862-870, 1998.
- 12) Osborne WR, Ramesh N, et al: Proc Natl Acad Sci USA 92, 8055-8058, 1995.
- 13) Nabel EG, Plautz G, et al: Science 244, 1342-1344, 1989.
- 14) Messina LM, Podrazik RM, et al: Proc Natl Acad Sci USA 89, 12018-12022, 1992.
- 15) Wilson JM, Birinyi LK, et al: Science 244, 1344-1346, 1989.
- 16) Dichek DA, Anderson J, et al: Circulation 93, 301-309, 1996.
- 17) Flugelman MY, Virmani R, et al: Circ Res 70, 348-354, 1992.
- 18) Koh GY, Kim S-J, et al: The J Clinical Investigation 95, 114-121, 1995.
- 19) Barr E, Leiden JM, et al: Science 254, 1507-1509, 1991.
- 20) Lee RJ, Springer ML, et al: Circulation 102, 898-901, 2000.
- 21) Yau TM, Fung k, et al: Circulation 104(suppl I), I-218-I-222, 2001.
- 22) Suzuki K, Murtuza B, et al: Circulation 104(suppl I), I-207-I-212, 2001.
- 23) Lu Y, Shansky J, et al: Circulation 104, 594-599, 2001.
- 24) Campbell AIM, Zhao Y, et al: Circulation 104, 2242-2248, 2001.
- 25) Iwaguro H, Yamaguchi J, et al: Circulation 105, 732-738, 2002.
- 26) Tabata Y, Ikada Y: J Pharm 39, 698-704, 1987.
- 27) Kasahara H, Tanaka E, et al: Journal of the American College of Cardiology, in press.
- 28) Nagaya N, Horio T, et al: Circulation 106(suppl II), II-496, 2002.

▶▶参考図書

- BME vol 16. No. 2特集 再生医療とMEの接点. 2002.
- 循環器科vol 51, No.3 循環器内科学における先進治療. 2002.

藤井隆文 (ふじいたかふみ)

(国立循環器病センター研究所心臓生理部)

- 1997年 岡山大学医学部卒業
- 岡山大学医学部心臓血管外科入局
- 1999年 呉共済病院心臓血管外科
- 2000年 社会保険広島市民病院心臓血管外科
- 2001年 国立病院岡山医療センター心臓血管外科
- 2002年 国立循環器病センター研究所心臓生理部

応用編

11章

再生医療とDOCS



## Controlled release of plasmid DNA from cationized gelatin hydrogels based on hydrogel degradation

Yasunori Fukunaka<sup>a,b</sup>, Kazunori Iwanaga<sup>a</sup>, Kazuhiro Morimoto<sup>c</sup>, Masawo Kakemi<sup>a</sup>,  
Yasuhiko Tabata<sup>b,\*</sup>

<sup>a</sup>Department of Pharmaceutics, Osaka University of Pharmaceutical Sciences, 4-20-1 Nasahara, Takatsuki, Osaka 569-1041, Japan

<sup>b</sup>Institute for Frontier Medical Sciences, Kyoto University, 53 Kawara-cho Shogoin, Sakyo-ku, Kyoto 606-8507, Japan

<sup>c</sup>Department of Pharmaceutics, Hokkaido University of Pharmaceutical Sciences, 7-1 Katsuraoka-cho, Otaru, Hokkaido 047-0264, Japan

Received 8 August 2001; accepted 18 January 2002

### Abstract

This paper shows achievement of the *in vivo* controlled release of a plasmid DNA from a biodegradable hydrogel and the consequent regulation of gene expression period. Cationization of gelatin was performed through introduction of ethylenediamine and the gelatin prepared was crosslinked by various concentrations of glutaraldehyde to obtain cationized gelatin (CG) hydrogels as the carrier of plasmid DNA. *In vivo* release of plasmid DNA from the CG hydrogels was compared with the *in vivo* degradation of hydrogels. When CG hydrogels incorporating <sup>125</sup>I-labeled plasmid DNA were implanted into the femoral muscle of mice, the plasmid DNA radioactivity remaining decreased with time and the retention period prolonged with a decrease in the water content of hydrogels used. The higher the water content of <sup>125</sup>I-labeled CG hydrogels, the faster the hydrogel radioactivity remaining decreased with time. The time profile of plasmid DNA remaining in the hydrogels was in good accordance with that of hydrogel radioactivity, irrespective of the water content. Intramuscular implantation of plasmid DNA-incorporated CG hydrogels enhanced significantly expression of the plasmid DNA around the implanted site. The retention period of gene expression became longer as the hydrogel water content decreased. Fluorescent microscopic study revealed that the plasmid DNA–CG complex was detected around the hydrogel implanted even after 7-day implantation in marked contrast to the injection of plasmid DNA solution. It was concluded that in our hydrogel system, active plasmid DNA was released accompanied with the *in vivo* degradation of hydrogel, resulting in extended gene expression. The time profile of plasmid DNA release and the consequent gene expression was controllable by changing the water content of hydrogels. © 2002 Elsevier Science B.V. All rights reserved.

**Keywords:** Plasmid DNA; Cationized gelatin hydrogel; Controlled release; Hydrogel degradation; Gene expression

### 1. Introduction

Recently, gene therapy has been increasingly clinically applied to cancer and congenital immunological diseases [1,2]. To this end, the vector for enhanced gene expression is needed and many

\*Corresponding author. Tel.: +81-75-751-4121; fax: +81-75-751-4144.

E-mail address: yasuhiko@frontier.kyoto-u.ac.jp (Y. Tabata).

researches have been performed to develop viral and non-viral vectors [3,4]. The former vector is widely used for clinical gene therapy because of the high efficiency of gene expression. However, there are some problems to be resolved, e.g., virus antigenicity. On the other hand, for the latter vector, less transfection efficiency than the viral vector is one of the largest issues, although it has advantages in terms of easy production, safety, and low cost. As trials to improve the efficiency, several technologies have been added for vector design and additional assistance, for instance application of electric and ultrasound stimuli [5–7]. Once the vector–plasmid DNA complex in the solution is injected into the body, gene expression cannot be always expected because of the easy diffusion away from the injected site. Thus, it is necessary as a trial for enhanced gene expression to achieve the controlled release of plasmid DNA over an extended time period by incorporating the plasmid DNA into a carrier. It is possible that controlled release technology enables the plasmid DNA to enhance the transfection probability at the applied site, resulting in promoted gene expression. It has been demonstrated that the release of plasmid DNA using biodegradable poly(lactic acid) augmented expression efficiency [8]. A collagen minipellet is reported to be effective in prolonging the period of gene expression [9]. However, little has been investigated on the effect of time period of plasmid DNA release on that of gene expression.

We have prepared a biodegradable hydrogel from gelatin as a release carrier of growth factors and succeeded in enhancing the *in vivo* biological activities of growth factor which cannot be always detected only by the administration in the solution form [10,11]. In this hydrogel system, the growth factor physicochemically immobilized in the hydrogel can be released only when the hydrogel is degraded to generate water-soluble gelatin fragments [12]. If this release system can be applied to plasmid DNA, it will be possible to achieve the controlled release based on hydrogel degradation. In this study, a cationized residue was introduced into gelatin to allow the plasmid DNA to electrostatically immobilize into the hydrogel-constituting gelatin.

The objective of the present study is to investigate whether or not the *in vivo* release of plasmid DNA is

achieved from biodegradable hydrogels of the cationized gelatin. Following implantation of cationized gelatin (CG) hydrogels incorporating a  $^{125}\text{I}$ -labeled plasmid DNA or  $^{125}\text{I}$ -labeled CG hydrogels into the femoral muscle of mice, the time profile of their radioactivity remaining was compared for CG hydrogels of different water contents. We examined the gene expression by the CG hydrogels incorporating plasmid DNA in the mouse muscle to compare it with the *in vivo* DNA retention in time duration. Retention of plasmid DNA as well as the gelatin constituting hydrogel in the muscle was also evaluated histologically.

## 2. Materials and methods

### 2.1. Materials

Gelatin was prepared through an acid process of pig skin type I collagen and kindly supplied by Nitta Gelatin (Osaka, Japan). Ethylenediamine, glutaraldehyde, 2,4,6-trinitrobenzenesulfonic acid,  $\beta$ -alanine, and protein assay kit (Lot No. L8900) were purchased from Nacalai Tesque (Kyoto, Japan) and used as obtained. As a coupling agent, 1-ethyl-3-(3-dimethylaminopropyl) carbodiimide hydrochloride salt (EDC) was obtained from Dojindo Laboratories (Kumamoto Japan). Rhodamine B isothiocyanate (RITC) and fluorescein isothiocyanate (FITC) were obtained from Sigma–Aldrich Japan (Tokyo, Japan). *N*-Succinimidyl-3-(4-hydroxy-3,5-di[ $^{125}\text{I}$ ]-iodophenyl) propionate ([ $^{125}\text{I}$ ]Bolton-Hunter Reagent, NEX-120H, 147 MBq/ml in anhydrous benzene) was purchased from NEN Research Products (DuPont, Wilmington, DE).

### 2.2. Preparation of cationized gelatin

Ethylenediamine and EDC were added into 250 ml of 100 mM phosphate-buffered solution containing 5 g of gelatin at a molar ratio to the carboxyl groups of gelatin of 50. Immediately after that, the pH of the solution was adjusted at 5.0 by adding 5 N of HCl. The reaction mixture was agitated at 37 °C for 18 h and then dialyzed against double-distilled water (DDW) for 48 h at 25 °C. The dialyzed solution was freeze-dried to obtain a cationized gelatin. The

percentage of amino groups introduced into gelatin was determined by the conventional trinitrobenzene sulfonate method [13]. When calculated based on the calibration curve prepared by using  $\beta$ -alanine, the percentage of cationized gelatin prepared was 47.8 mol/mol carboxyl groups of gelatin.

### 2.3. Preparation of cationized gelatin hydrogels

An aqueous solution of 10 wt% cationized gelatin (800  $\mu$ l) was cast into a polytetrafluoroethylene mold (2 $\times$ 2 cm<sup>2</sup>, 0.8 mm depth), and left at 4 °C overnight for gelation. Cationized gelatin (CG) hydrogels were crosslinked in HCl–acetone (3:7, v/v) containing various amounts of glutaraldehyde. The crosslinking reaction was allowed to proceed for 24 h at 4 °C and the resulting hydrogel sheets were then immersed in 100 mM glycine aqueous solution at 4 °C for 24 h to block the residual aldehyde groups of glutaraldehyde. The hydrogel sheets were cut out to obtain hydrogel discs (5 $\times$ 5 $\times$ 1 mm<sup>3</sup>) and rinsed three times with DDW at 4 °C and freeze-dried. The freeze-dried hydrogels were sterilized by ethylene oxide gas. No change in hydrogel shape was observed before and after freeze-drying and sterilization processes.

It is known that the *in vivo* degradability of gelatin hydrogels by enzyme depends on their extent of crosslinking, which enables regulation by changing the glutaraldehyde concentration in hydrogel preparation [14]. However, it is difficult from the viewpoint of polymer sciences to directly determine the crosslinking extent of hydrogels. Thus, generally the water content of hydrogels is measured to evaluate their crosslinking extent, because the two values correlate well with each other [15]. In this study, the water content of cationized gelatin hydrogels prepared was determined as a measure to compare them in terms of crosslinking extent. After the freeze-dried hydrogel was swollen at 37 °C for 24 h in phosphate-buffered saline solution (PBS, pH 7.4), the weight of swollen hydrogel ( $W_s$ ) was measured. The weight of freeze-dried hydrogel ( $W_d$ ) was measured and the water content, which was defined by  $((W_s - W_d) / W_s) \times 100$  [11], was calculated from the  $W_s$  and  $W_d$  values. When the glutaraldehyde concentration was changed in hydrogel preparation, the water content of CG hydrogels prepared ranged from 96.4 to 99.7

Table 1  
Characterization of cationized gelatin hydrogels prepared

Code	Concentration of cationized gelatin (wt%)	Concentration of glutaraldehyde ( $\mu$ g/ml)	Water content (wt%)
CG 1	10	31.3	96.4
CG 2	10	0.78	97.4
CG 3	10	0.31	98.3
CG 4	10	0.16	99.7

wt% (Table 1). The CG hydrogel is a sponge with an average pore size of 500  $\mu$ m, as shown in Fig. 1. The inner structure was similar, irrespective of the hydrogel water content (data not shown).

### 2.4. Radiolabeling of cationized gelatin hydrogels

CG hydrogels prepared were radioiodinated using [<sup>125</sup>I]Bolton-Hunter reagent. Briefly, 100  $\mu$ l of [<sup>125</sup>I]Bolton-Hunter reagent solution in anhydrous benzene was bubbled with dry nitrogen gas until benzene evaporation was completed. Then, 125  $\mu$ l of 0.1 M sodium borate-buffered solution (pH 8.5) was added to the dried reagent, followed by pipetting to prepare aqueous [<sup>125</sup>I]Bolton-Hunter solution. The freeze-dried discs of CG hydrogels were impregnated with prepared aqueous solution at a volume of 20  $\mu$ l per disc. The resulting swollen hydrogel discs were kept at 4 °C for 3 h to introduce <sup>125</sup>I residues into the amino groups of gelatin. The radioiodinated CG hydrogel discs were rinsed with DDW by exchanging it periodically at 4 °C for 4 days to exclude non-coupled, free <sup>125</sup>I-labeled reagent from <sup>125</sup>I-labeled gelatin hydrogels. When measured periodically, the radioactivity of DDW returned to the background level after rinsing for 3 days. No shape change of swollen hydrogels was observed during radiolabeling and the subsequent rinsing process, irrespective of the hydrogel water content. Finally, the resulting swollen hydrogel discs were freeze-dried.

### 2.5. DNA isolation

The plasmid DNA used was the expression vector consisting of the coding sequence of LacZ and a SV40 promoter inserted at the upstream (pSV-LacZ,

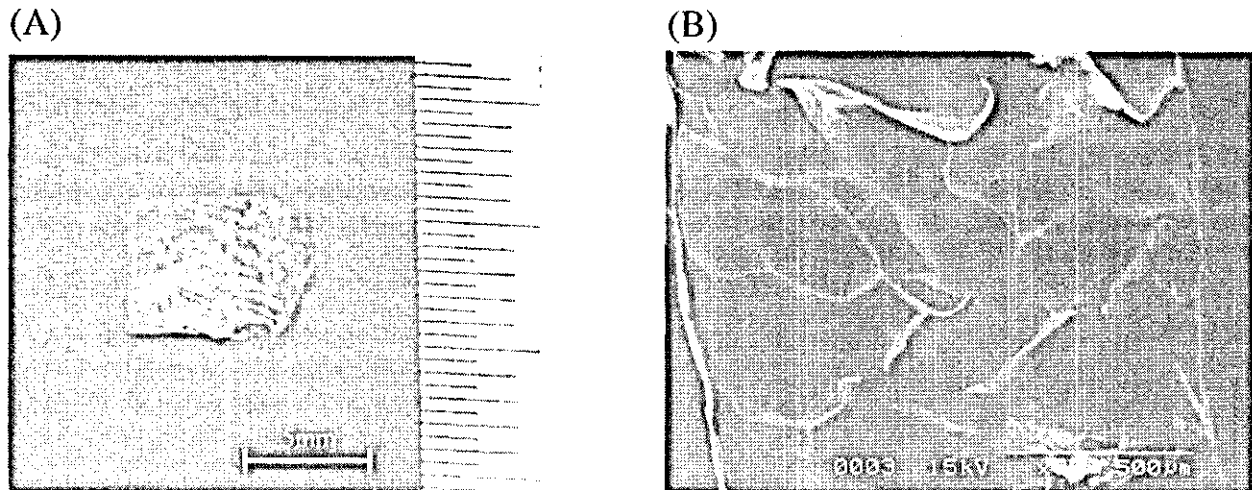


Fig. 1. Optical (A) and scanning electron microscopic photographs (B) of CG 2 hydrogels.

7931 bp). The pSV-LacZ was prepared from bacterial cultures with Qiagen Maxi kit (Qiagen, Tokyo, Japan). Briefly, the *Escherichia coli* transformants containing pSV-LacZ were grown by incubating in Luria-Bertani (LB) medium (Invitrogen Japan, Tokyo, Japan) at 37 °C for 16 h. Following harvest of bacterial cells by centrifugation (6000×g, 15 min, 4 °C), the bacterial pellet was suspended in a resuspension buffer (50 mM Tris-HCl, 10 mM EDTA, pH 8.0) in the presence of RNase (100 μg/ml) and lysed in a lysis buffer (200 mM NaOH, 1% sodium dodecyl sulfate). The lysate was neutralized by addition of 3.0 M potassium acetate solution (pH 5.5), filtered, and applied to the Qiagen syringe of anion-exchange resin. The Qiagen syringe was rinsed with a medium-salt buffer (1 M NaCl, 50 mM MOPS, pH 7.0, and 15% isopropyl alcohol) to remove remaining contaminants, such as traces of RNA and protein. The plasmid DNA was then eluted with an elution buffer (1.25 M NaCl at pH 8.5, 50 mM Tris-HCl, and 15% isopropyl alcohol) and precipitated by addition of isopropyl alcohol. After centrifugation at 15 000×g for 10 min at 4 °C, the pellet was washed with 70% ethanol aqueous solution to remove residual salt and to substitute the solvent. The DNA centrifuged was properly air-dried and dissolved in a small volume of TE buffer (10 mM Tris-HCl and 1 mM EDTA). The absorbance ratio at the wavelength of 260–280 nm was mea-

sured for evaluation of plasmid purity to be between 1.8 and 2.0.

#### 2.6. Radiolabeling of pSV-LacZ

PBS containing 2.5 mg/ml of pSV-LacZ (1.0 ml) was added to the dried [<sup>125</sup>I]Bolton-Hunter reagent prepared by the method mentioned previously. The resulting solution was kept at 37 °C overnight to introduce <sup>125</sup>I residue into the amino groups of pSV-LacZ. Non-coupled, free <sup>125</sup>I-labeled reagent was removed from <sup>125</sup>I-labeled pSV-LacZ solution by gel filtration with a PD 10 column (Amersham-Pharmacia Biotech, Tokyo, Japan).

#### 2.7. Preparation of CG hydrogels incorporating pSV-LacZ

Impregnation of pSV-LacZ into freeze-dried CG hydrogels was carried out using PBS containing 100 μg of pSV-LacZ. pSV-LacZ-free, empty CG hydrogels were prepared in a similar way except for using pSV-LacZ-free PBS. Briefly, 20 μl of PBS with or without pSV-LacZ were dropped onto the dried hydrogel discs and left at 4 °C overnight to obtain CG hydrogels incorporating pSV-LacZ or those without pSV-LacZ incorporation. The pSV-LacZ solution was fully sorbed into the dried CG hydrogels during the swelling process because the solution

volume was much less than that theoretically impregnated into each hydrogel, irrespective of the water content of hydrogels. Similarly, an aqueous solution of  $^{125}\text{I}$ -labeled pSV-LacZ was sorbed into freeze-dried CG hydrogel discs to prepare CG hydrogels incorporating  $^{125}\text{I}$ -labeled pSV-LacZ. Every hydrogel disc prepared by this procedure had similar appearance, irrespective of the hydrogel water content, radiolabeling, or preparation conditions.

### 2.8. Estimation of *in vivo* degradation of CG hydrogels

$^{125}\text{I}$ -Labeled CG hydrogels with different water contents were implanted into the femoral muscle of ddY mice, 6–7 weeks old (Shizuoka Animal Center, Shizuoka, Japan). At 1, 3, 7, 10, 14, and 21 days after hydrogel implantation, the mouse muscle containing the implanted hydrogels ( $1 \times 1 \times 1 \text{ cm}^3$ ) was taken out to measure their radioactivity on a gamma counter (ARC-301B, Aloka, Tokyo, Japan). The radioactivity ratio of the muscle sample to the hydrogel implanted initially was measured to express the percentage of remaining activity in the hydrogels. For each experimental group, three mice were sacrificed at each time point for *in vivo* evaluation unless otherwise mentioned. All the animal experiments were carried out according to the Institutional Guidance of Kyoto University on Animal Experimentation.

### 2.9. Estimation of *in vivo* pSV-LacZ release from CG hydrogels incorporating pSV-LacZ

Following implantation of  $^{125}\text{I}$ -labeled pSV-LacZ-incorporated CG hydrogels with different water contents into the femoral muscle of mice at different time intervals, the mouse muscles containing cationized gelatin hydrogels were taken out. As control, the solution of  $^{125}\text{I}$ -labeled pSV-LacZ in PBS was injected into the femoral muscle ( $100 \mu\text{l}/\text{site}$ ). The radioactivity of the muscle samples was measured on the gamma counter and the ratio to the initial radioactivity of hydrogels or pSV-LacZ solution injected was expressed as the percentage of radioactivity remaining.

### 2.10. *In vivo* assessment of gene expression following implantation of CG hydrogels incorporating pSV-LacZ

pSV-LacZ-incorporated CG hydrogels with different water contents were implanted into the femoral muscle of mice. As a control,  $100 \mu\text{l}$  of pSV-LacZ solution was intramuscularly injected into the mouse. The pSV-lacZ dose was  $100 \mu\text{g}/\text{mouse}$  and six mice were used at each time point for every experimental group. The mice were sacrificed 1, 3, 7, 14, and 21 days after pSV-lacZ treatment to evaluate gene expression.

For evaluation of gene expression at the treated muscle,  $\beta$ -galactosidase activity was measured by use of Invitrogen kit (Invitrogen, USA). Briefly, the muscle samples were immersed and homogenized in the lysis buffer ( $0.1 \text{ M Tris-HCl}$ ,  $2 \text{ mM EDTA}$ ,  $0.1\% \text{ Triton X-100}$ ) at the lysis buffer volume (ml)/sample weight (mg) ratio of 4:1 in order to normalize the influence of weight variance on the  $\beta$ -galactosidase assay. The sample lysate ( $2 \text{ ml}$ ) was transferred to a centrifuge tube, followed by freeze-and-thaw three times and centrifugation at  $15\,000 \times g$  at  $4^\circ\text{C}$  for 5 min. The supernatant ( $30 \mu\text{l}$ ) was mixed with  $70 \mu\text{l}$  of aqueous solution containing  $4 \text{ mg/ml } o\text{-nitrophenyl } \beta\text{-D-galactopyranoside (ONPG)}$  and  $200 \mu\text{l}$  of cleavage buffer ( $60 \text{ mM Na}_2\text{HPO}_4\text{-}7\text{H}_2\text{O}$ ,  $40 \text{ mM NaH}_2\text{PO}_4\text{-H}_2\text{O}$ ,  $10 \text{ mM KCl}$ , and  $1 \text{ mM MgSO}_4\text{-}7\text{H}_2\text{O}$ ,  $\text{pH } 7$ ) in a fresh microcentrifuge tube. After incubation at  $37^\circ\text{C}$  for 30 min,  $500 \mu\text{l}$  of  $1 \text{ M sodium carbonate solution}$  was added to the solution mixture. The solution absorbance was measured at the wavelength of  $420 \text{ nm}$  to evaluate the  $\beta$ -galactosidase activity. The number of muscle samples was four for each experimental group.

### 2.11. Fluorescent labeling of CG hydrogels

CG hydrogels were fluorescently labeled according to the method previously reported [16]. Briefly,  $20 \mu\text{l}$  of  $10 \text{ mg/ml FITC}$  solution in  $0.2 \text{ M sodium carbonate-buffered solution (pH } 9.7)$  was dropped onto the freeze-dried CG hydrogel disc. The resulting swollen hydrogel discs were left at  $4^\circ\text{C}$  for overnight for fluorescent labeling. The FITC labeled CG hydrogels were rinsed with  $0.2 \text{ M sodium}$

carbonate-buffered solution (pH 9.7) by exchanging it periodically at 4 °C for 4 days to exclude non-coupled, free FITC from FITC-labeled CG hydrogels. Shape of swollen hydrogels was not changed during fluorescent-labeling and the subsequent rinsing process, irrespective of the hydrogel water content. Finally, the resulting swollen hydrogels were freeze-dried.

### 2.12. Fluorescent labeling of pSV-LacZ

The coupling reaction of RITC to pSV-LacZ was carried out by mixing the two substances in 0.2 M sodium carbonate-buffered solution (pH 9.7) both at a concentration of 1 mg/ml at 4 °C overnight, followed by gel filtration with a PD 10 column (Amersham-Pharmacia) to obtain an RITC-labeled pSV-LacZ.

### 2.13. Fluorescent microscopic observation

FITC-labeled CG hydrogels incorporating RITC-labeled pSV-LacZ were prepared by the same procedure mentioned above and implanted into the femoral muscle of mice. As control, the solution of RITC-labeled pSV-lacZ in 0.2 M sodium carbonate-buffered solution (pH 9.7) was injected into the femoral muscle (100  $\mu$ l/site). The mouse muscle containing the implanted hydrogels was taken out 1, 3, and 7 days after hydrogel implantation and embedded in Tissue-Tek (OCT compound, Miles, USA). Their cryosections (8  $\mu$ m thickness) were prepared from the embedded sample to view the localization of CG-pSV-LacZ complex by double-fluorescent staining pattern on Olympus AX-80 fluorescence microscope equipped with an Olympus DP50 digital camera (KS Olympus, Tokyo, Japan).

### 2.14. Statistical analysis

All the data were analyzed by Students' *t*-test and results were expressed as means  $\pm$  standard error of the means (S.E.M.). Statistical significance was accepted at  $P < 0.05$ .

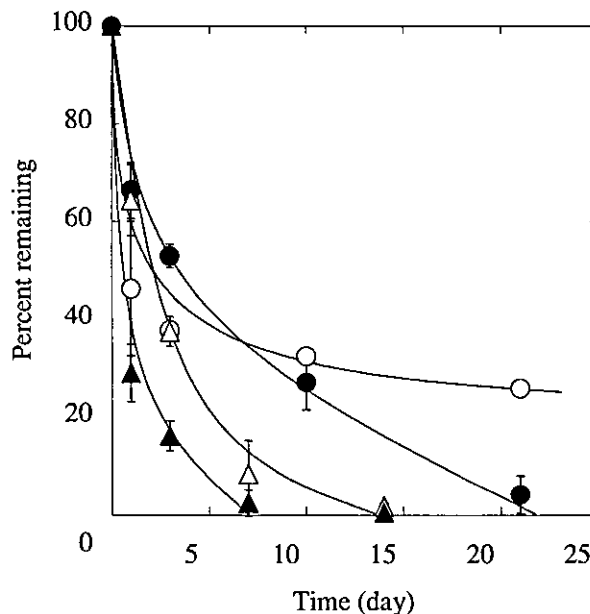


Fig. 2. The time course of the radioactivity remaining of  $^{125}$ I-labeled CG 1 (○), CG 2 (●), CG 3 (△), and CG 4 hydrogels (▲) after implantation into the femoral muscle of mice (initial weight of the wet hydrogel=0.2 g). The number of CG hydrogels used for every experiment is three.

## 3. Results

### 3.1. In vivo degradation profile of CG hydrogels

Fig. 2 shows the time course of radioactivity remaining after implantation of  $^{125}$ I-labeled CG hydrogels into the femoral muscle of mice. The radioactivity remaining in CG hydrogels implanted decreased with time for every hydrogel sample, but the hydrogels with lower water contents retained the radioactivity for longer time periods than that of hydrogels with higher water contents.

### 3.2. In vivo release profile of pSV-LacZ

Fig. 3 shows the decrement patterns of pSV-LacZ radioactivity after implantation of CG hydrogels incorporating  $^{125}$ I-labeled pSV-LacZ into the femoral muscle of mice. The residual radioactivity of pSV-LacZ in CG hydrogels decreased with implantation time and the decrement pattern of radioactivity greatly depended on the water content of CG hydro-

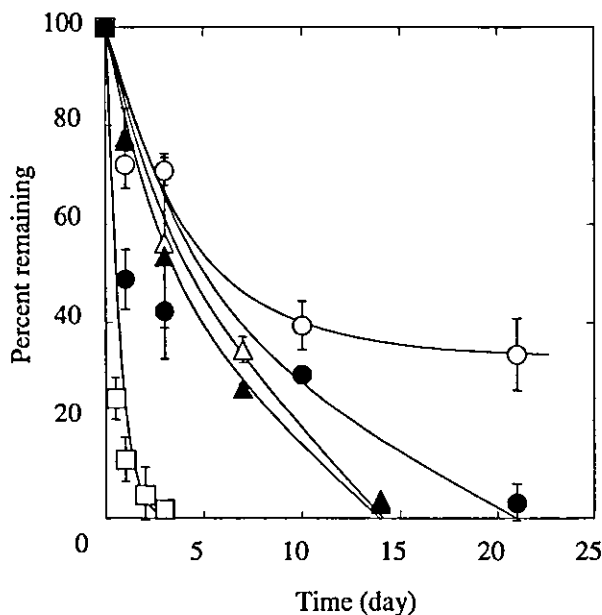


Fig. 3. The time course of the radioactivity remaining of CG 1 (○), CG 2 (●), CG 3 (△), and CG 4, hydrogels incorporating  $^{125}\text{I}$ -labeled pSV-lacZ after implantation into the femoral muscle of mice. (□) The radioactivity remaining after the intramuscular injection of  $^{125}\text{I}$ -labeled pSV-LacZ in the solution form. The number of CG hydrogels used for every experiment is three.

gels. The lower the water content of hydrogels, the longer their radioactivity retention in hydrogels. On the contrary, for free  $^{125}\text{I}$ -labeled pSV-LacZ the radioactivity rapidly disappeared from the injected site within 3 days.

### 3.3. Relationship of radioactivity remaining between pSV-LacZ and CG hydrogels

Fig. 4 shows the pSV-LacZ radioactivity remaining plotted as a function of the radioactivity remaining of  $^{125}\text{I}$ -labeled CG hydrogels remaining. The radioactivity remaining of pSV-LacZ depended on that of CG hydrogels. Irrespective of the hydrogel water content, the former value increased with an increase in the latter one. Interestingly, the percentage of pSV-LacZ remaining tended to be large upon comparing with that of the corresponding CG hydrogel remaining.

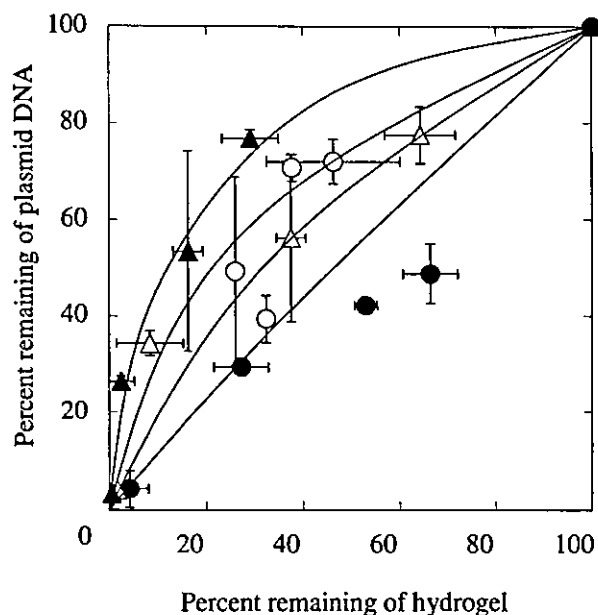


Fig. 4. The radioactivity remaining of CG hydrogels incorporating  $^{125}\text{I}$ -labeled pSV-LacZ plotted against that of  $^{125}\text{I}$ -labeled CG hydrogels after implantation into the femoral muscle of mice: (○) CG 1, (●) CG 2, (△) CG 3, and (▲) CG 4 hydrogels. The number of CG hydrogels used for every experiment is three.

### 3.4. Time course of gene expression

Fig. 5 shows the time course of gene expression following intramuscular implantation of CG hydrogels incorporating pSV-LacZ or injection of PBS containing pSV-LacZ. The water contents of CG hydrogels used were 97.4 and 98.3 wt%. The injection of the pSV-LacZ solution showed significant gene expression only at 3 days after injection and thereafter the expression return to the basal level. The level of gene expression was not enhanced by implantation of pSV-LacZ-free, empty CG hydrogels. On the contrary, both of the CG hydrogels incorporating pSV-LacZ enhanced significantly the expression level as well as prolonged the duration time period. The level of gene expression increased within 3 days after implantation of the hydrogels with the water content of 98.3 wt% and the level became maximal 7 days after implantation, followed by return to the basal level at Day 14. On the other hand, the hydrogels with the water content of 97.4 wt% enable the time period of gene expression to

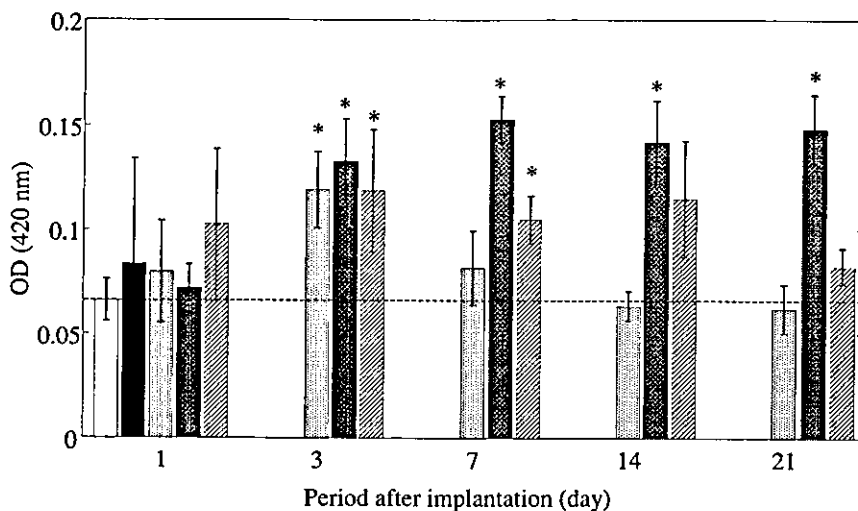


Fig. 5. The time course of LacZ gene expression after implantation of CG hydrogels incorporating pSV-LacZ into the femoral muscle of mice: (□) pSV-LacZ-free CG 2 hydrogel, (■) pSV-LacZ-free CG 3 hydrogel, (▨) pSV-LacZ solution, and (▩) CG 2 and (▧) CG 3 hydrogels incorporating pSV-LacZ. The pSV-LacZ dose is 100  $\mu\text{g}/\text{mouse}$  muscle. A dotted line indicates the level of gene expression in the femoral muscle of untreated, normal mice. The number of CG hydrogels used for every experiment is three. \* $P < 0.05$ : significant against the OD value of untreated, normal mice.

maintain for a longer period than those with the higher water content although the similar onset of the initial effect was observed for both the hydrogels.

### 3.5. Histological observation of mouse muscle receiving implantation of CG hydrogels incorporating pSV-LacZ

Fig. 6 shows fluorescent microscopic photographs of muscles 1, 3, and 7 days after implantation of FITC-labeled CG hydrogels incorporating RITC-labeled pSV-LacZ. Irrespective of time after implantation, the fluorescent staining of pSV-LacZ around the implanted site of hydrogels coincided in position with that of CG. On the contrary, no fluorescent image was detected over the time range studies after the injection of RITC-labeled pSV-LacZ solution.

## 4. Discussion

Generally, gelatin is not degraded by simple hydrolysis but by proteolysis. Therefore, in this

study, degradation of CG hydrogels was carried out in the mouse muscle to obtain the time profile of their radioactivity loss in vivo. As is apparent from Fig. 2, CG hydrogels with the water content of 98.3 wt% were degraded with time and completely disappeared in the mouse muscle on day 14. This degradation rate of 98.3 wt% hydrogel was middle between those of hydrogels with water contents of 97.4 and 99.7 wt%, indicating that in vivo degradation of gelatin hydrogels is mainly governed by their water content alone. This phenomenon is similar to that observed for non-cationized gelatin hydrogels [12].

As shown in Fig. 3, the remaining radioactivity of pSV-LacZ incorporated in implanted CG hydrogels decreased with time and the decrement rate was higher for the hydrogels of higher water content. The decrement pattern of hydrogel radioactivity was correlated with that of pSV-lacZ radioactivity, irrespective of the hydrogel water content (Fig. 4). This result suggests the possibility that pSV-LacZ was released from the CG hydrogel in the body as a result of biodegradation of hydrogel. It seems probable that pSV-LacZ molecules, once ionically complexed with the cationized gelatin, cannot be released

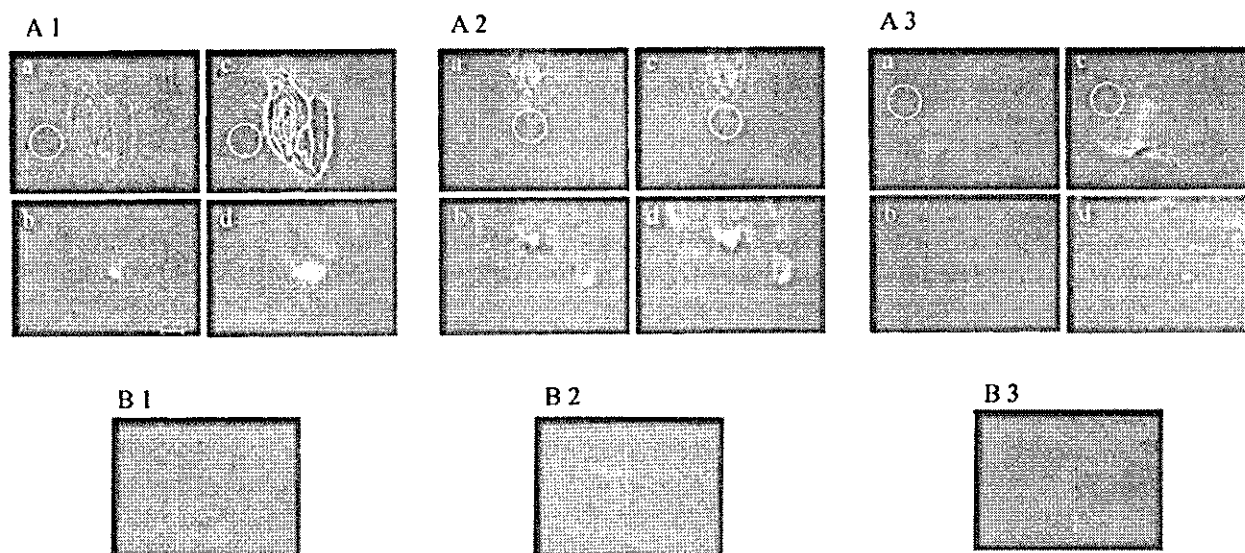


Fig. 6. Fluorescent microscopic photographs of histological sections of mouse femoral muscle 1 (A1,B1), 3 (A2,B2), and 7 days (A3,B3) after intramuscular implantation of FITC-labeled CG 2 hydrogels incorporating RITC-labeled pSV-LacZ (A) or intramuscular injection of RITC-labeled pSV-LacZ in the solution form (B). The localization of pSV-LacZ and CG hydrogel is fluorescently discriminated by red and green colors. The left (a,b) and right pictures (c,d) in the A1, A2, and A3 show the tissue localization of pSV-LacZ and CG hydrogel, respectively. The (b) and (d) pictures are the magnified images at the circle site of (a) and (c) pictures which is around the hydrogel implanted. The fluorescent image of (a) and (c) pictures in A1, A2, and A3 indicate the localization of pSV-LacZ and CG, respectively. The superposition between the two images implies that the pSV-LacZ is present being complexed with CG molecules.

from the CG hydrogel unless hydrogel degradation takes place. It is likely that the pSV-LacZ molecules are released from the hydrogels with being complexed with degraded gelatin fragments of positive charge. This is experimentally suggested from the double staining image of pSV-LacZ and cationized gelatin around the hydrogel implanted in fluorescent observation (Fig. 6). Since the pSV-LacZ itself is negatively charged, it will be expected to ionically complex with the cationized gelatin. If the pSV-LacZ-cationized gelatin complex has a positive charge, the charge will promote the internalization of the pSV-LacZ into cells because the charge of cell surface is negative. Probably, such a complex formation would facilitate the transfection of pSV-LacZ, resulting in gene expression. Moreover, it is expected that the continuous presence of complex at a certain body site by the controlled release system results in promoted gene expression there. The mechanism of gene expression by the present release system of plasmid DNA should be clarified by further investigation.

Higher remaining percentage of pSV-LacZ than that of CG hydrogel may be explained in terms of polyion complexation between the pSV-LacZ and CG molecules. For the experiment of *in vivo* hydrogel degradation, the pSV-LacZ-unloaded CG hydrogels are used. It is highly possible that the loading of pSV-LacZ affects the hydrogel degradation. Since the presence of plasmid DNA allows cationized gelatin molecules to electrostatically crosslink to each other, probably the plasmid DNA-loaded hydrogel will be degraded slowly compared with the plasmid DNA-unloaded hydrogel. As a result, the difference in the radioactivity remaining between the pSV-LacZ and CG hydrogel would be observed. Another possibility is: based on the possible release mechanism, the pSV-LacZ will be released while being complexed with the CG to have a positive charge. Considering the electric charge in the body, the surface of the cells as well as the glycosaminoglycan present in the extracellular matrix is negative. It is conceivable that the pSV-LacZ-cationized gelatin complexes released are ionically trapped by

the negatively charged substances, resulting in the prolonged remaining in the body.

The crosslinking extent of CG hydrogels influences not only the water content but also the biodegradation of hydrogels. Slower degradation of CG hydrogel with lower water contents is undoubtedly due to larger extent of crosslinking. The present study demonstrated that pSV-LacZ was released from the cationized gelatin hydrogel as a result of biodegradation of CG, because the pSV-LacZ molecules ionically complexed with crosslinked gelatin will be released only when water-soluble gelatin fragments are generated through biodegradation of gelatin hydrogels. The prolonged period of gene expression by the pSV-LacZ incorporated hydrogel of lower water content, shown in Fig. 5, is ascribed to slower hydrogel degradation. The gene expression induced by the pSV-LacZ-incorporated hydrogel with the water content of 98.3 wt% disappeared at approximately 14 days. At the same time, the hydrogel was completely degraded *in vivo* and the pSV-LacZ remaining was almost zero. On the other hand, the gelatin hydrogel with a water content as low as 97.4 wt% still exhibited significant gene expression at the 21th day after implantation, while the hydrogel remaining was observed at the implantation site. At that time, the pSV-LacZ was also retained in the remaining hydrogel, as shown in Fig. 5. This finding strongly suggests that the pSV-LacZ incorporated in CG hydrogels still maintains its transfection activity even though exposed to *in vivo* environment for a long time period. Probably, the controlled release will enable the pSV-LacZ not only to increase the local concentration but also to prolong the period of enhanced concentration at the implanted site of hydrogels. It is highly conceivable that such advantages enhance the possibility of pSV-LacZ to transfect, resulting in promoted and prolonged gene expression.

The present study is the first report that the period of gene expression could be changed by altering that of plasmid DNA release. Since the plasmid DNA released is complexed with the cationized gelatin, this complexation functions positively for the transfection into cells. In this system, the plasmid DNA release can be regulated only by changing the hydrogel degradability which is controllable by regulating the crosslinking extent of hydrogel. This

implies that, irrespective of the shape of release carriers, controlled release can be achieved even if the hydrogel carrier is as small as injectable. The present release concept based on polyion complexation may be applicable to any type of plasmid DNA. This release system is being presently applied to the plasmid DNA coding a growth factor to demonstrate the *in vivo* efficient exertion of the biological activity.

## References

- [1] D.T. Curiel, W.R. Gerritsen, M.R. Krul, Progress in cancer gene therapy, *Cancer Gene Ther.* 7 (8) (2000) 1197–1199.
- [2] A. Fischer, S. Haccin-Bey, F. Le Deist, C. Soudais, J.P. Di Santo, G. de Saint Basile, M. Cavazzana-Calvo, Gene therapy of severe combined immunodeficiencies, *Immunol. Rev.* 178 (2000) 13–20.
- [3] G. Romano, P. Michell, C. Pacilio, A. Giordano, Latest developments in gene transfer technology: achievements, perspectives, and controversies over therapeutic applications, *Stem Cells* 18 (1) (2000) 19–39.
- [4] D. Luo, W.M. Saltzman, Synthetic DNA delivery systems, *Nat. Biotechnol.* 18 (1) (2000) 33–37.
- [5] K. Anwer, G. Kao, B. Proctor, I. Ansonme, V. Florack, R. Earls, E. Wilson, T. McCreery, E. Unger, A. Rolland, S.M. Sullivan, Ultrasound enhancement of cationic lipid-mediated gene transfer to primary tumors following systemic administration, *Gene Ther.* 7 (2000) 1833–1839.
- [6] H. Hossein, T. Aoyama, O. Ogawa, Y. Tabata, Ultrasound enhancement of *in vitro* transfection of plasmid DNA by a cationized gelatin. *J. Drug Target* (2001) in press.
- [7] H. Aihara, J. Miyazaki, Gene transfer into muscle by electroporation *in vivo*, *Nat. Biotechnol.* 16 (1998) 867–870.
- [8] D. Luo, K. Woodrow-Mumford, N. Belcheva, W.M. Saltzman, Controlled DNA delivery systems, *Pharm. Res.* 16 (8) (1999) 1300–1308.
- [9] T. Ochiya, Y. Takahama, S. Nagahara, Y. Sumita, A. Nishida, H. Itoh, Y. Nagai, M. Terada, New delivery system for plasmid DNA *in vivo* using atelocollagen as a carrier material: the Minipellet, *Nat. Med.* 5 (6) (1999) 707–710.
- [10] K. Yamada, Y. Tabata, K. Yamamoto, S. Miyamoto, I. Nagata, H. Kikuchi, Y. Ikada, Potential efficacy of basic fibroblast growth factor incorporated in biodegradable hydrogels for skull bone regeneration, *J. Neurosurg.* 86 (1997) 871–875.
- [11] Y. Tabata, S. Hijikata, Y. Ikada, Enhanced vascularization and tissue granulation by basic fibroblast growth factor impregnated in gelatin hydrogels, *J. Control. Release* 31 (1994) 189–199.
- [12] Y. Tabata, A. Nagano, Y. Ikada, Biodegradation of hydrogel carrier incorporating fibroblast growth factor, *Tissue Eng.* 5 (2) (1999) 127–138.

- [13] S.L. Snyder, P.Z. Sobocinski, An improved 2,4,6-trinitrobenzenesulfonic acid method for the determination of amines, *Anal. Biochem.* 64 (1975) 284–288.
- [14] Y. Tabata, Y. Ikada, Vascularization effect of basic fibroblast growth factor released from gelatin hydrogels with different biodegradabilities, *Biomaterials* 20 (1999) 2169–2175.
- [15] P.J. Flory, Swelling of network structure, in: *Principles of Polymer Chemistry*, Cornell University Press, New York, 1953, pp. 576–581.
- [16] Y. Kato, H. Onishi, Y. Machida, Biological characteristics of lactosaminated *N*-succinyl-chitosan as a liver-specific drug carrier in mice, *J. Control. Release* 70 (3) (2001) 295–307.

# Endothelial Progenitor Cell Vascular Endothelial Growth Factor Gene Transfer for Vascular Regeneration

Hideki Iwaguro, MD; Jun-ichi Yamaguchi, MD, PhD; Christoph Kalka, MD; Satoshi Murasawa, MD, PhD; Haruchika Masuda, MD, PhD; Shin-ichiro Hayashi, MD, PhD; Marcy Silver, BS; Tong Li, MD; Jeffrey M. Isner, MD; Takayuki Asahara, MD, PhD

**Background**—Previous studies have established that bone marrow–derived endothelial progenitor cells (EPCs) are present in the systemic circulation. In the current study, we investigated the hypothesis that gene transfer can be used to achieve phenotypic modulation of EPCs.

**Methods and Results**—In vitro, ex vivo murine vascular endothelial growth factor (VEGF) 164 gene transfer augmented EPC proliferative activity and enhanced adhesion and incorporation of EPCs into quiescent as well as activated endothelial cell monolayers. To determine if such phenotypic modulation may facilitate therapeutic neovascularization, heterologous EPCs transduced with adenovirus encoding VEGF were administered to athymic nude mice with hindlimb ischemia; neovascularization and blood flow recovery were both improved, and limb necrosis/autoamputation were reduced by 63.7% in comparison with control animals. The dose of EPCs used for the in vivo experiments was 30 times less than that required in previous trials of EPC transplantation to improve ischemic limb salvage. Necropsy analysis of animals that received DiI-labeled VEGF-transduced EPCs confirmed that enhanced EPC incorporation demonstrated in vitro contributed to in vivo neovascularization as well.

**Conclusions**—In vitro, VEGF EPC gene transfer enhances EPC proliferation, adhesion, and incorporation into endothelial cell monolayers. In vivo, gene-modified EPCs facilitate the strategy of cell transplantation to augment naturally impaired neovascularization in an animal model of experimentally induced limb ischemia. (*Circulation*. 2002;105:732-738.)

**Key Words:** gene therapy ■ endothelium ■ angiogenesis ■ ischemia

Previous studies from our laboratory<sup>1–6</sup> and others<sup>7–13</sup> have established that bone marrow–derived endothelial progenitor cells (EPCs) are present in the systemic circulation, are augmented in response to certain cytokines and/or tissue ischemia, and home to as well as incorporate into sites of neovascularization. More recently, EPCs have been investigated as therapeutic agents; in these studies of “supply-side angiogenesis,” EPCs harvested from the peripheral circulation have been expanded ex vivo and then administered to animals with limb<sup>14</sup> or myocardial<sup>15</sup> ischemia to successfully enhance neovascularization. Physiological evidence of neovascular function in these preclinical animal models includes a high rate of limb salvage and improvement in myocardial function.

### See p 672

EPC transplantation thus constitutes a novel therapeutic strategy that could provide a robust source of viable endothelial cells (ECs) to supplement the contribution of ECs resident in the adult vasculature that migrate, proliferate, and remodel in response to angiogenic cues, according to the

classic paradigm of angiogenesis developed by Folkman and colleagues.<sup>16</sup> Just as classic angiogenesis may be impaired in certain pathological phenotypes,<sup>17–20</sup> however, aging, diabetes, hypercholesterolemia, and hyperhomocysteinemia may likewise impair EPC function, including mobilization from the bone marrow and incorporation into neovascular foci. Gene transfer of EPCs during ex vivo expansion constitutes a potential means of addressing such putative liabilities in EPC function. Moreover, phenotypic modulation of EPCs ex vivo may also reduce the number of EPCs required for optimal transplantation after ex vivo expansion and thus serve to address a practical limitation of EPC transplantation, namely the volume of blood required to extract an optimal number of EPCs for autologous transplantation.

Accordingly, we investigated the hypothesis that gene transfer can be used to achieve phenotypic modulation of EPCs. In particular, we sought to determine the impact of vascular endothelial growth factor (VEGF) gene transfer on certain properties of EPCs in vitro and the consequences of VEGF EPC-gene transfer on neovascularization in vivo.

Received October 12, 2001; revision received November 29, 2001; accepted December 14, 2001.

From the Division of Cardiovascular Research and Medicine (H.I., J.Y., C.K., S.M., H.M., S.H., M.S., T.L., J.M.I., T.A.), St Elizabeth's Medical Center, Tufts University School of Medicine, Boston, Mass; and the Department of Physiology (H.I.) and Institute of Medical Science (T.A.), Tokai University School of Medicine, Japan.

Correspondence to Takayuki Asahara, MD, PhD, St Elizabeth's Medical Center, 736 Cambridge St, Boston, MA, 02135. E-mail asa777@aol.com  
© 2002 American Heart Association, Inc.

*Circulation* is available at <http://www.circulationaha.org>

DOI: 10.1161/hc0602.103673

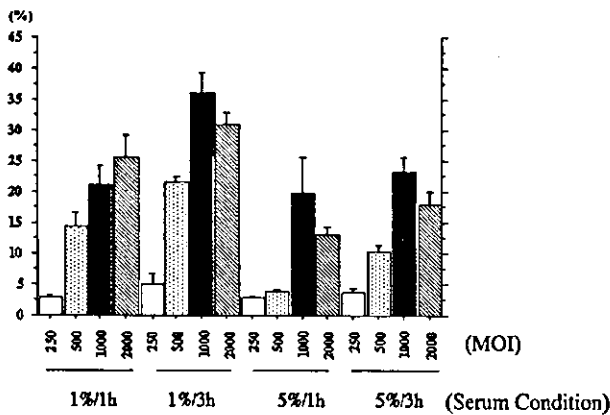


**Figure 1.** Profile of transfection efficiencies for Ad/ $\beta$ gal in ex vivo-expanded human EPCs. Four different multiplicities of infection (MOI, 250, 500, 1000, and 2000) were tested in 2 different media conditions (1% or 5% serum EBM-2) for 1 or 3 hours of incubation. Error bars represent SEM of triplicate experiments. After these preliminary experiments, human EPCs were transduced with 1000 MOI Ad/VEGF or Ad/ $\beta$ gal for 3 hours in 1% serum media.

## Methods

### EPC Culture

Ex vivo expansion of EPC was performed as recently described.<sup>14</sup> In brief, peripheral blood mononuclear cells from human volunteers were plated on human fibronectin-coated (Sigma) culture dishes and maintained in EC basal medium-2 (EBM-2) (Clonetics) supplemented with 5% fetal bovine serum, human VEGF-A, human fibroblast growth factor-2, human epidermal growth factor, insulin-like growth factor-1, and ascorbic acid. After 4 days in culture, nonadherent cells were removed by washing, new media was applied, and the culture maintained through day 7.

### EPC Gene Transfer

After 7 days in culture, cells were transduced with an adenovirus encoding the murine VEGF 164 gene (Ad/VEGF) or lacZ gene (Ad/ $\beta$ gal) (generously provided by Kevin Peters).<sup>21</sup> To establish optimum conditions for EPC adenovirus gene transfer serum concentration, virus incubation time and virus concentration were evaluated (Figure 1). After preliminary experiments were performed, human EPCs were transduced with 1000 MOI Ad/VEGF or Ad/ $\beta$ gal for 3 hours in 1% serum media. After transduction, cells were washed with PBS and incubated with EPC media for 24 hours before transplantation.

### Proliferative Activity Assay

At 24 hours after gene transfer, EPCs transduced with Ad/VEGF (Td/V-EPCs), Ad/ $\beta$ -gal (Td/ $\beta$ -EPCs), or nontransduced EPCs (non-Td/EPCs) were reseeded on 96-well plates coated with human fibronectin for assay of proliferative activity with the use of the MTS [3-(4,5-dimethylthiazol-2-yl)-5-(3-carboxymethoxyphenyl)-2-(4-sulfophenyl)-2H-tetrazolium] Assay (Promega). After 48 hours in culture, MTS/PMS (phenazine methosulfate) solution was added to each well for 3 hours, and light absorbance at 490 nm was detected by ELISA plate reader (Bionetics Laboratory).

### In Vitro Incorporation of Td-EPCs Into Human Umbilical Vein Endothelial Cell Monolayer

At 24 hours after gene transfer, Td/V-EPCs and Td/ $\beta$ -EPCs were stained with fluorescent carbocyanine DiI (Biomedical Technologies). DiI-labeled EPCs were incubated on a monolayer of human umbilical vein endothelial cells (HUVECs) in 4-well culture slides with or without pretreatment of tumor necrosis factor (TNF)- $\alpha$

(1ng/mL) for 12 hours.<sup>22</sup> Three hours after incubation, nonadherent cells were removed by washing with PBS, new media was applied, and the culture was maintained for an additional 24 hours. The total number of adhesive EPCs in each well was counted in a blinded manner under a  $\times 200$  magnification field of a fluorescent microscope.

### Td-EPCs Transplantation Animal Model

All procedures were performed in accordance with the St Elizabeth's Institutional Animal Care and Use Committee. Female athymic nude mice (Jackson Laboratory, Bar Harbor, Maine), 8 to 9 weeks old and 17 to 20 g weight, were anesthetized with 160 mg/kg IP pentobarbital for operative resection of one femoral artery<sup>23</sup> and subsequently for laser Doppler perfusion imaging.

As a preliminary experiment, we performed dose-dependent EPC transplantation to determine the minimum number of VEGF-transduced EPCs that was required to achieve a magnitude of therapeutic neovascularization similar to that which could be achieved with nontransduced EPCs. According to this result,  $1.5 \times 10^4$  VEGF-transduced EPCs, 30 times less than the number required for cell therapy alone, were used in the current series of in vivo experiments. One day after unilateral femoral artery excision,  $1.5 \times 10^4$  Td/V-EPCs ( $n=11$ ), Td/ $\beta$ -EPCs ( $n=11$ ), or non-Td/EPCs ( $n=5$ ) in 100  $\mu$ L EBM-2 media without growth factors were administered through the tail vein.

To track the fate of transplanted EPCs, 4 mice in each EPC cohort received EPCs that were marked with the fluorescent carbocyanine DiI dye (Molecular Probes). In brief, before cellular transplantation, EPCs in suspension were washed with PBS and incubated with DiI at a concentration of 2.5  $\mu$ g/mL PBS for 5 minutes at 37°C and 15 minutes at 4°C. After two washing steps in PBS, the cells were resuspended in EBM-2 medium. At 30 minutes before the animals were killed, a subgroup ( $n=4$  each group) of mice received an intravenous injection of 50  $\mu$ g of Bandeiraea simplicifolia lectin 1 (BS-1) conjugated with FITC (Vector Laboratories).

### Plasma VEGF Levels

To confirm that the Ad/VEGF could mediate successful gene transfer at the protein level, an enzyme-linked immunoassay (ELISA, R&D System) was used to quantify VEGF levels in plasma from animals 1, 4, 7, and 28 days after intravenous injections of Td/V-EPCs or Td/ $\beta$ -EPCs. The results were compared with a standard curve constructed with murine VEGF (each assay carried out in duplicate for each animal). Absorbance was measured at 450 nm by means of a microplate reader.

### Physiological Assessment of Animals Given Transplantation

Laser Doppler perfusion imaging (LDPI) (Moor Instruments) was used to record blood flow measurements on day 0 and day 28 after surgery, as previously described. In these digital color-coded images, red hue indicates regions with maximum perfusion, medium perfusion values are shown in yellow, and lowest perfusion values are represented as blue. The resulting images display absolute values in readable units. For quantification, the ratio of readable units in ischemic to nonischemic hindlimb is determined.

### Histological Assessment of Animals Given Transplantation

Vascular density was evaluated at the microvascular level through the use of light microscopic sections harvested from the ischemic hindlimbs at necropsy. Tissue sections from the lower calf muscles of ischemic limbs were harvested on days 7 and 28. Muscle samples were embedded in OCT compound (Miles), snap-frozen in liquid nitrogen, and cut into 5- $\mu$ m-thick sections. Tissue sections were stained for alkaline phosphatase with an indoxyltetrazolium method to detect capillary endothelial cells as previously described<sup>23</sup> and then were counterstained with eosin. A total of 20 different fields were randomly selected, and the number of capillaries and myofibers were counted ( $\times 40$  magnification for 20 fields).

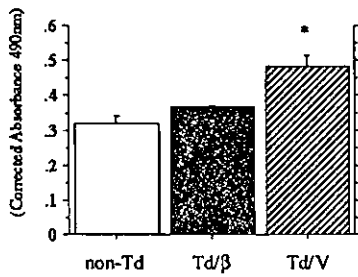


**Figure 2.** Proliferative activity assay. Proliferative activity of EPCs transduced in 5% serum was measured by MTS assay after 48 hours in culture. Increase in mitogenic response of EPCs transduced with Ad/VEGF (Td/V-EPCs) was statistically significant in comparison with EPCs transduced with Ad/βgal (Td/β-EPCs) and nontransduced EPCs (non-Td). \* $P < 0.01$  vs Td/βgal and non-Td.

**Statistical Analysis**

All results are expressed as mean ± SEM. Statistical significance was evaluated by means of a paired Scheffé *t* test or ANOVA. A value of  $P < 0.05$  was considered to denote statistical significance.

**Results**

**Proliferative Activity Assay**

MTS assay was used to determine proliferative activity of transduced EPCs. With the use of 5% serum-conditioned media, proliferative activity of Ad/VEGF-transduced EPCs exceeded proliferative activity of Ad/β-gal ( $0.48 \pm 0.03$  versus  $0.37 \pm 0.01$  corrected absorbance at 490 nm,  $P < 0.01$ ) and nontransduced EPCs (non-Td =  $0.32 \pm 0.02$ ,  $P < 0.05$ ) in vitro (Figure 2).

**In Vitro Incorporation of Td-EPCs Into HUVEC Monolayer**

At 24 hours after transduction, EPCs were labeled with the fluorescent marker DiI for cell tracking. DiI-labeled, VEGF-transduced EPCs were incubated on a HUVEC monolayer with or without TNF-α (1 ng/mL) pretreatment for 12 hours (Figure 3A). After 3 hours of incubation, nonadherent cells were removed by washing with PBS, and DiI-marked cells adherent to the HUVEC monolayer were manually counted. In the quiescent HUVEC monolayer, adhesion of DiI-labeled EPCs was not significantly different between Td/V-EPCs and Td/β-EPC ( $2.7 \pm 0.2$  versus  $2.2 \pm 0.3$ ,  $P = NS$ ) (Figure 3B). In activated HUVECs, however, adhesion of DiI-labeled Td/V-EPCs exceeded Td/β-EPCs ( $4.3 \pm 0.4$  versus  $2.9 \pm 0.3$ ,  $P < 0.01$ ).

Alternatively, the same cells were incubated in new media and maintained for 24 hours on the HUVEC monolayer to confirm incorporation in vitro. In the quiescent HUVEC monolayer, incorporation of DiI-labeled Td/V-EPCs exceeded Td/β-EPCs ( $7.0 \pm 0.5$  versus  $3.5 \pm 0.5$ ,  $P < 0.01$ ) (Figure 3B). In activated HUVECs, incorporation of DiI-labeled Td/V-EPCs also exceeded Td/β-EPCs ( $13.8 \pm 0.8$  versus  $5.3 \pm 0.6$ ,  $P < 0.001$ ).

**Transgene Expression After Td/V-EPC Transplantation**

Ad/VEGF-mediated gene transfer and expression were confirmed by ELISA assay of plasma samples obtained from

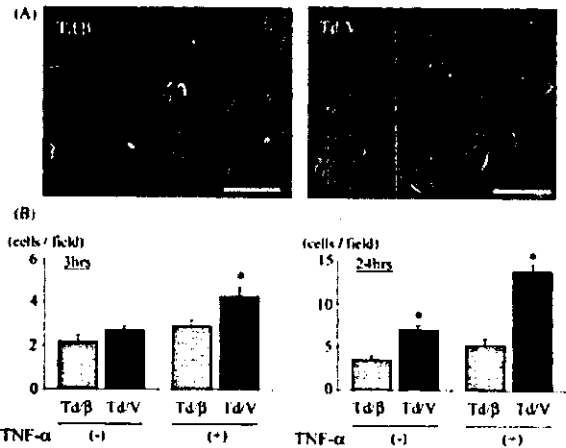


**Figure 3.** In vitro incorporation of Td-EPCs on HUVEC monolayer. A, Representative macroscopic photographs of Td/V-EPCs and Td/β-EPCs on HUVEC monolayer 24 hours after transduction with Ad/VEGF or Ad/βgal, respectively. Left panel shows Td/β-EPCs; right panel, Td/V-EPCs on HUVEC monolayer, in each case pretreated with TNF-α stimulation. White bars indicate 50-μm length. B, Quantitative analysis of EPC adhesion observed 3 hours and incorporation observed 24 hours after transduction with (+) and without (-) pretreatment of TNF-α. \* $P < 0.01$  vs Td/β-EPCs.

mice after Td/V-EPC transplantation. Mice transplanted with Td/V-EPCs disclosed significantly higher VEGF protein levels (day 1,  $828.18 \pm 8.84$  versus  $4.56 \pm 2.21$  pg/mL; day 4,  $421.27 \pm 12.60$  versus  $5.16 \pm 2.79$  pg/mL; day 7,  $65.65 \pm 3.20$  versus  $3.78 \pm 2.26$  pg/mL; day 28,  $17.40 \pm 1.99$  versus  $4.42 \pm 1.88$  pg/mL;  $P < 0.01$ ) at each time point than did mice transplanted with Td/β-EPCs (Figure 4).

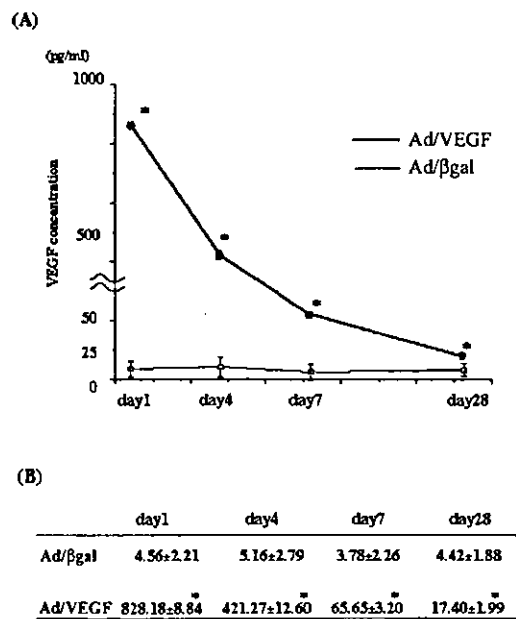


**Figure 4.** VEGF plasma levels after administration of Td/V-EPCs and Td/β-EPCs. A, Quantification of VEGF expression was measured by ELISA assay at each time point (days 1, 4, 7, and 28). B, table of results. \* $P < 0.01$  vs Td/β-EPCs.

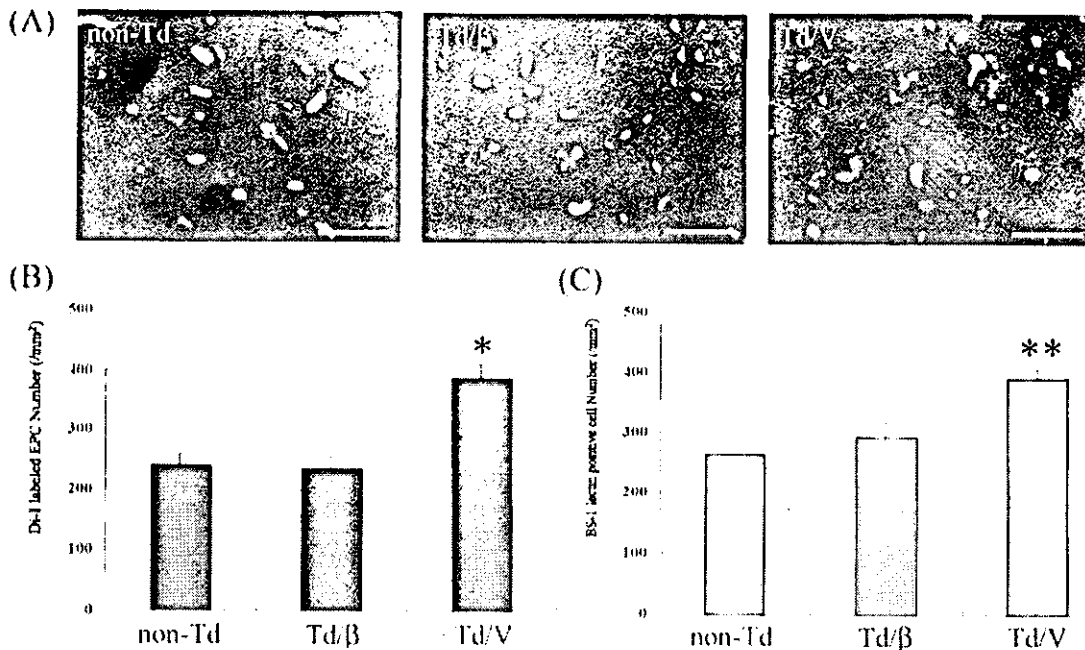


**Figure 5.** Histological identification of EPC incorporation in vivo. Transplanted human DiI-labeled, EPC-derived cells were identified by red fluorescence in histological sections retrieved from ischemic muscle. Host mouse vasculature was identified by green fluorescence in the same tissue sections. Td/V-EPC-transplanted animals had increased numbers of EPC-derived vasculature as well as mouse vasculature compared with control animals (Td/β-EPC and non-Td groups). White bars indicate 100- $\mu$ m length. A, Transplanted EPC-derived vasculature and mouse vasculature were quantified for the same light microscopic fields. Density of DiI-labeled EPCs in tissue sections of skeletal muscle removed from ischemic limb was greater in the Td/V-EPCs group than either of the other two groups (B). Density of BS-1 lectin-positive vasculature in tissue sections of skeletal muscles removed from the ischemic limb was also greater in the Td/V-EPCs group than either of the other 2 groups (C). \* $P < 0.001$  vs non-Td and Td/β-EPCs, \*\* $P < 0.01$  vs non-Td and Td/β-EPCs.

### EPC Incorporation Into Ischemic Hindlimb

Transplanted human EPC derived cells marked with DiI were identified in tissue sections by red fluorescence. In contrast, the mouse vasculature, stained by premortem administration of BS-1 lectin, was identified by green fluorescence in the same tissue sections. Td/V-EPC-transplanted animals disclosed increased numbers of DiI-labeled, red fluorescent EPC-derived vasculature as well as mouse vasculature versus control groups (Td/β-EPC and non-Td group) (Figure 5A).

Both transplanted EPC-derived vasculature and mouse vasculature were analyzed quantitatively in the same microscopic field. The density of DiI-labeled EPCs in tissue sections of hindlimb muscles was greater in the Td/V-EPC group ( $389 \pm 23$  mm<sup>2</sup>) than either of the other two groups (non-Td/EPCs =  $241 \pm 18$  mm<sup>2</sup>; Td/β-EPCs =  $236 \pm 20$  mm<sup>2</sup>,  $P < 0.001$ ) at day 7 (Figure 5 B). The density of BS-1 lectin-positive vasculature in sections of skeletal muscle removed from the ischemic limb was also greater in the Td/V-EPC group ( $391 \pm 16$  mm<sup>2</sup>) than the other two groups (non-Td/EPCs =  $263 \pm 18$  mm<sup>2</sup>; Td/β-EPCs =  $292 \pm 26$  mm<sup>2</sup>,  $P < 0.01$ ) at day 7 (Figure 5C).

### Physiological Assessment of Animals Given Transplantation

The impact of human gene-modified EPC administration on neovascularization was investigated in a murine model of hindlimb ischemia. One day after operative excision of one femoral artery, athymic nude mice ( $n = 27$ ), in which angiogenesis is characteristically impaired,<sup>14,21</sup> received an intra-

venous injection of  $1.5 \times 10^4$  transduced EPCs (Td/V-EPCs,  $n = 11$ ) or Td/β-EPCs ( $n = 11$ ). As additional control animals, 5 mice with hindlimb ischemia were identically injected with non-Td/EPCs. Enhanced neovascularization in mice transplanted with Td/V-EPCs led to important biological consequences, compared with control animals.

After administration of Td/β-EPCs to 11 mice, 3 (27.2%) had extensive toe necrosis, and the remaining 8 (72.7%) underwent autoamputation of the ischemic limb (Figure 6A). In contrast, Td/V-EPC transplantation was associated with successful limb salvage in 7 (63.6%) of 11 animals; toe necrosis was limited to 3 (27.2%) mice, and only 1 (9%) had spontaneous limb amputation (Figure 6B).

Serial examination of hindlimb perfusion by LDPI was performed at days 0 and 28 (Figure 7A). The ratio of ischemic/normal blood flow in mice transplanted with Td/V-EPCs indicated significantly greater hindlimb perfusion compared with those mice transplanted with Td/β-EPCs and nontransduced EPCs at day 28 ( $0.71 \pm 0.15$  versus  $0.40 \pm 0.03$  versus  $0.34 \pm 0.04$ ,  $P < 0.05$ ) (Figure 7B).

### Histological Assessment of Animals Given Transplantation

To further evaluate the impact of EPC gene transfer on revascularization of the ischemic hindlimb, histological examination of skeletal muscle sections retrieved from the ischemic hindlimbs of mice killed at day 28 was performed as described above. Capillary density observed in the mice transplanted with Td/V-EPCs was significantly higher than in